

Article

Cyclic CH₄ Injection for Enhanced Oil Recovery in the Eagle Ford Shale Reservoirs

Yuan Zhang ^{1,*}, Yuan Di ², Yang Shi ³ and Jinghong Hu ¹

¹ Beijing Key Laboratory of Unconventional Natural Gas Geology Evaluation and Development Engineering, China University of Geosciences (Beijing), Beijing 100083, China; hujinghong@cugb.edu.cn

² College of Engineering, Peking University, Beijing 100871, China; diyuan@mech.pku.edu.cn

³ Research Institute of Petroleum Exploration and Development, PetroChina, Beijing 100083, China; shy312@petrochina.com.cn

* Correspondence: zhangyuan@cugb.edu.cn; Tel.: +86-151-2007-7038

Received: 24 October 2018; Accepted: 7 November 2018; Published: 9 November 2018



Abstract: Gas injection is one of the most effective enhanced oil recovery methods for the unconventional reservoirs. Recently, CH₄ has been widely used; however, few studies exist to accurately evaluate the cyclic CH₄ injection considering molecular diffusion and nanopore effects. Additionally, the effects of operation parameters are still not systematically understood. Therefore, the objective of this work is to build an efficient numerical model to investigate the impacts of molecular diffusion, capillary pressure, and operation parameters. The confined phase behavior was incorporated in the model considering the critical property shifts and capillary pressure. Subsequently, we built a field-scale simulation model of the Eagle Ford shale reservoir. The fluid properties under different pore sizes were evaluated. Finally, a series of studies were conducted to examine the contributions of each key parameter on the well production. Results of sensitivity analysis indicate that the effect of confinement and molecular diffusion significantly influence CH₄ injection effectiveness, followed by matrix permeability, injection rate, injection time, and number of cycles. Primary depletion period and soaking time are less noticeable for the well performance in the selected case. Considering the effect of confinement and molecular diffusion leads to the increase in the well performance during the CH₄ injection process. This work, for the first time, evaluates the nanopore effects and molecular diffusion on the CH₄ injection. It provides an efficient numerical method to predict the well production in the EOR process. Additionally, it presents useful insights into the prediction of cyclic CH₄ injection effectiveness and helps operators to optimize the EOR process in the shale reservoirs.

Keywords: Cyclic CH₄ injection; enhanced oil recovery; nanopore confinement; molecular diffusion; sensitivity analysis

1. Introduction

As reported, around 40% of the natural gas reserves are contained in the unconventional reservoirs all over the world [1]. The Eagle Ford shale is one of the productive oil shale reservoirs in the North America, which is located in the northwest of Texas. The main thickness of production varies from 50 to 300 feet [2,3]. The technologies of horizontal drilling and multistage hydraulic fracturing have attracted much attention, especially for the micro- and nano-pores in the unconventional reservoirs [4,5]. The combination of these technologies is extensively used to exploit the reserves in the tight and shale reservoirs [6,7]. However, Dejam et al. [8,9] pointed out that low permeability may increase the threshold pressure gradient, and large amount of oil still reserves in the formations, which requires gas injection for the production enhancement [10–12].

Due to the low permeability of shale rocks, waterflooding cannot perform as effective as that in the conventional resources. Hence, the attention has been attracted to gas injection in the unconventional reservoirs. Recent theoretical and experimental studies have shown that CH₄ injection is more impressive than CO₂ because it has high compressibility and the sources are rich [13,14]. Therefore, CH₄ can take the place of CO₂ in some situations. Alfarge et al. [15] pointed out that extending soaking period and increasing injection volume are benefit to improve the well production. Meng and Sheng [16] conducted the experiment of CH₄ Huff-n-Puff injection in the core samples, confirming that condensate recovery increase by 6% in the Huff-n-Puff injection operation. However, most studies focus on the primary depletion production; the physical mechanisms on the effectiveness of cyclic CH₄ injection are still limited.

Literatures have reported the evaluation of gas injection in shale oil reservoirs [15,17–19]. Sigmund et al. [20] and Brusilovsky [21] have conducted experiments in the porous media. They concluded that the phase behavior in the porous media deviates from the bulk phase. Recent studies have shown that nanopore confinement is an important factor since the nanopores cause high capillary pressure, affecting the properties of components as well as phase behavior further theoretically and experimentally [22–25]. Wang et al. [26] and Nojabaei et al. [23] modified the vapor-liquid phase equilibrium model based on Young-Laplace equation and Leverett J-function. They then incorporated the phase equilibrium model into the reservoir simulator to predict the well production in the tight oil reservoirs. Yang et al. [27] modified the Peng-Robison equation of state and introduced a new term representing the molecule-wall interaction. They reproduced the collected data with an overall error of 7.64% compared to the molecular simulation results. Nanofluidic devices were applied to investigate the nanopore effects. Luo et al. [28] and Alfi et al. [29] conducted the nanofluidic experiment and they all concluded that the bubble point shifts with the effect of confinement. Salahshoor et al. [1] reviewed the mathematical models and experimental studies to compare the phase behavior in conventional reservoirs and tiny pores.

Molecular diffusion is another key mechanism affecting the gas injection effectiveness. Yu et al. [30] has investigated that molecular diffusivity should be correctly included in the simulation model. In the process of CO₂-CH₄ displacement, diffusion is also an important mechanism [31]. Zhang et al. [32] compared the oil recovery of CO₂-EOR process and concluded that considering molecular diffusion is beneficial to improve the oil recovery. However, these investigations only focus on the CO₂ injection process; the impact on the CH₄ injection was not well understood. Recent studies have concluded that the diffusion coefficient of CH₄ is on the same order of CO₂ [33,34]; hence, the effect of molecular diffusion needs to be well examined.

Figure 1 shows the sketch of CH₄ injection process in the fractured horizontal well. As CH₄ is injected, the molecules will move into the fractures and diffuse into the matrix. The fluid phase behavior in nanopores should be determined. Due to the nanopore effects, the injected components will not distribute homogenous among different sizes of pores. Additionally, it will result in different swelling effect in the gas injection from conventional reservoirs because of the confined phase behavior in nanopores.

From the literature survey, there are still some limitations behind the previous studies. Although the EOR process is efficient in the tight oil reservoirs, few studies focus on the effect of confinement on the EOR effectiveness, especially for the CH₄ injection. Additionally, most of previous studies analyzed the operation parameters and the investigation of physical mechanisms affecting the CH₄ injection is limited. In order to fill this gap, we proposed a useful method incorporating the phase behavior model into the compositional simulator, which can accurately and efficiently evaluate the effect of key parameters on the CH₄ injection effectiveness. This work systematically analyzes the physical mechanisms and operation parameters; it can be easily used in the operations of EOR process.

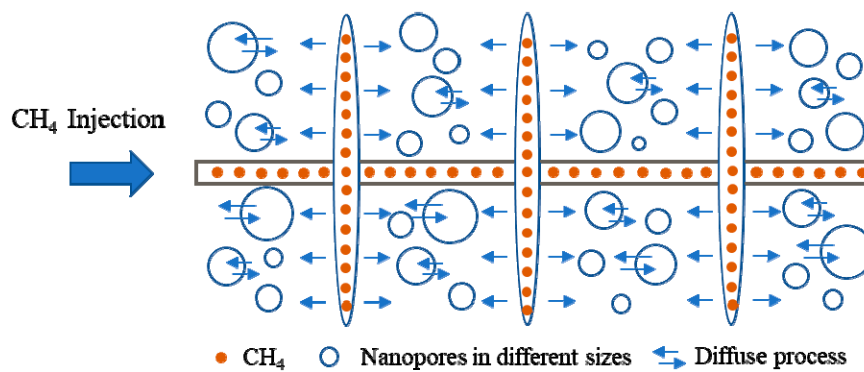


Figure 1. The sketch of CH₄ injection process in the fractured horizontal well (CH₄ molecules diffuse into different nanopores).

In this work, we evaluated the effect of confinement and CH₄ molecular diffusion on the cyclic CH₄ injection in the Eagle Ford shale reservoir. First, the methodology and detailed procedure were explained. Then, we built a reservoir model based on the fluid properties from the published Eagle Ford data [35]. The pore size distribution was obtained from the Eagle Ford rock samples [24]. Afterwards, a series of sensitivity analysis were performed to identify the impacts of the physical mechanisms on the effectiveness of cyclic CH₄ injection. Finally, we conducted the sensitivity analysis including operation parameters and physical mechanisms. This work provides a better analysis and optimization of CH₄ injection in the Eagle Ford shale reservoir.

2. Methodology

2.1. Shifts of Critical Properties

The nanopore effect on the critical temperatures and pressures has been reported in the literatures [24,36,37]. The interaction between the molecules and the pore walls is significant when the pore size is less than 10 nm [38,39]. In our study, the correlations published by Singh et al. [36] were applied to describe the critical property shifts [40]:

$$\Delta T_c^* = \frac{T_{cb} - T_{cp}}{T_{cb}} = 0.9409 \frac{\sigma_{LJ}}{r_p} - 0.2415 \left(\frac{\sigma_{LJ}}{r_p} \right)^2, \quad (1)$$

$$\Delta P_c^* = \frac{P_{cb} - P_{cp}}{P_{cb}} = 0.9409 \frac{\sigma_{LJ}}{r_p} - 0.2415 \left(\frac{\sigma_{LJ}}{r_p} \right)^2, \quad (2)$$

$$\sigma_{LJ} = 0.244 \sqrt[3]{\frac{T_{cb}}{P_{cb}}}, \quad (3)$$

where r_p represents the pore-throat radius, ΔT_c^* and ΔP_c^* express the relative critical temperature and pressure shift, respectively. T_{cb} and P_{cb} are the bulk critical temperature and pressure, respectively. T_{cp} and P_{cp} are the critical temperature and critical pressure in the confined space, respectively. σ_{LJ} is the Lennard-Jones size parameter (collision diameter).

2.2. Phase Equilibrium Calculation Considering Nanopore Confinement

In order to include the effect of confinement in the phase equilibrium model, the criterion of phase equilibrium can be rewritten as:

$$f_L^i(T, P_L, x_i) = f_V^i(T, P_V, y_i), \quad i = 1, \dots, N_c, \quad (4)$$

$$P_V - P_L = P_{cap}, \quad (5)$$

where f_L^i and f_V^i express the fugacity of component i in the liquid and vapor phases, respectively. T is the reservoir temperature. P_V and P_L represent the pressures of the vapor and liquid phase, respectively. P_{cap} is the capillary pressure in the confined space, which is calculated using the Young-Laplace equation [41], defining as:

$$P_{cap} = \frac{2\sigma \cos \theta}{r_p}, \tag{6}$$

where θ represents the contact angle. In this model, the contact angle is assumed as zero and the angle between organic and inorganic pores was neglected. The interfacial tension, σ is calculated using the following equation:

$$\sigma = \left[\sum_i^{N_C} (\bar{\rho}_L [P]_i x_i - \bar{\rho}_V [P]_i y_i) \right]^4, \tag{7}$$

where $\bar{\rho}_L$ and $\bar{\rho}_V$ denote density of the liquid and vapor phases, respectively. $[P]_i$ is the parachor of component i . Parachor of pure component and mixture can be obtained from the work by Pedersen and Christensen [42].

The Peng-Robinson equation of state [43] is modified as Equation (8) considering the effect of confinement:

$$P = \frac{RT}{V_m - b} - \frac{a\alpha}{V_m^2 + 2bV_m - b^2}, \tag{8}$$

where V_m and R represent the mole volume of component i and the universal gas constant, respectively. a and b are the parameters obtained by van der Waals mixing rules.

When the confinement is included, Equation (8) should be solved separately for liquid and vapor phases:

$$(Z_L)^3 - (1 - B_L)(Z_L)^2 + (A_L - 2B_L - 3(B_L)^2)Z_L - (A_L B_L - (B_L)^2 - (B_L)^3) = 0, \tag{9}$$

$$(Z_V)^3 - (1 - B_V)(Z_V)^2 + (A_V - 2B_V - 3(B_V)^2)Z_V - (A_V B_V - (B_V)^2 - (B_V)^3) = 0, \tag{10}$$

where $A_L = \frac{a_L \alpha P_L}{R^2 T^2}$, $B_L = \frac{b_L P_L}{RT}$, $A_V = \frac{a_V \alpha P_V}{R^2 T^2}$, $B_V = \frac{b_V P_V}{RT}$. Z_L and Z_V are the compressibility of liquid and vapor phases, respectively. The non-linear equations are solved by Newton-Raphson method. The roots of Equations (9) and (10) are determined with the criterion of Gibbs free energy minimization in the liquid and vapor phases.

In the following section, we first built a reservoir model based on the typical fluid and fracture properties, and then performed sensitivity analysis of different parameters in the cyclic CH₄ injection. The fluid properties considering the nanopore effects were calculated through the phase equilibrium model. Afterwards, the properties were implemented into the reservoir simulator of CMG to evaluate the cyclic CH₄ injection effectiveness [44]. The detailed workflow of this work is presented in Figure 2.

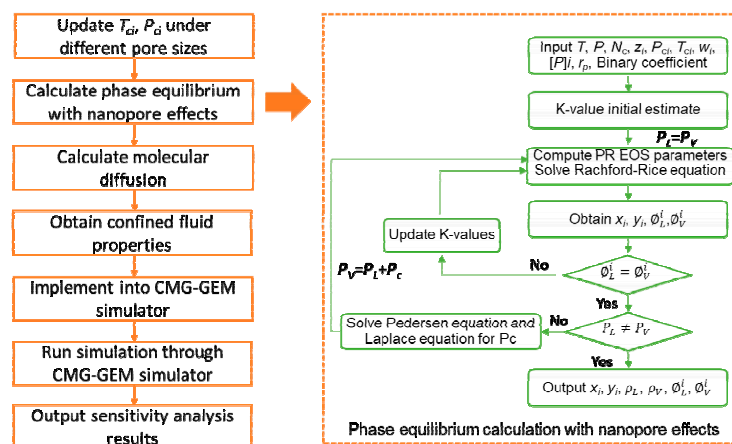


Figure 2. The workflow of evaluation of CH₄ injection effectiveness.

3. Base Case

In the simulation study, we set up the reservoir model using the CMG-GEM simulator [44]. The domain of the model is: 7785 ft in x direction, 1300 ft in y direction, and 40 ft in z direction. A horizontal well was set in the middle of the reservoir model, along with 76 hydraulic fractures. The fracture spacing is 80 ft and the fracture half-length is 210 ft. As reported, the reservoir temperature is 270 °F, the matrix porosity is 12%, and the initial reservoir pressure is 8125 psi. Table 1 summarizes the reasonable rock and fluid properties in the Eagle Ford shale reservoir [45]. The reservoir model is shown in Figure 3. Mohebbinia and Wong [46] have pointed out that molecular diffusion would be dominated in the low-permeability fractured reservoirs when gravitational drainage is inefficient. Hence, only diffusion mechanism was included in this work. The relative permeability curves are shown in Figure 4.

Table 1. Rock and fluid properties used in the reservoir model.

Properties	Value	Unit
Initial reservoir pressure	8125	psi
Reservoir temperature	270	°F
Reservoir thickness	100	ft
Water saturation	17%	-
Porosity	12%	-
Average matrix permeability	0.001	mD
Fracture half-length	210	ft
Fracture spacing	80	ft

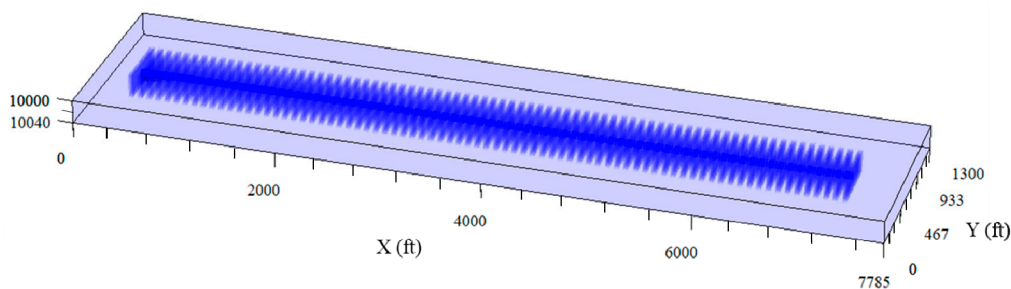


Figure 3. The reservoir simulation model in the cyclic CH₄ injection.

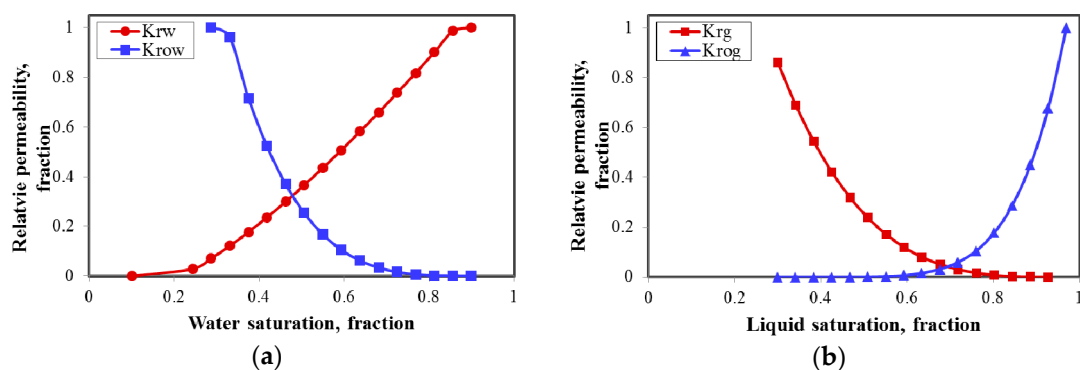


Figure 4. Relative permeability curves: (a) Water-oil relative permeability curve; (b) Liquid-gas relative permeability curve [38].

In this study, the fluid in the Eagle Ford reservoir is assumed containing six pseudo-components. Properties and binary interaction coefficients are listed in Tables 2 and 3, respectively. Oil gravity of 41 °API, gas-oil ratio of 1000 scf/stb, and formation volume factor of 1.65 rb/stb are obtained after tuning process. These properties have shown good agreements with the work by Orangi et al. [47].

Table 2. Properties of Eagle Ford oil modified from Orangi et al. [47].

Components	Mole Fraction (%)	Critical Temperature (K)	Critical Pressure (atm)	Acentric Factor	Molecular Weight (g/mol)
CO ₂	1.18	304.20	72.8	0.225	44.01
N ₂	0.16	126.20	33.5	0.040	28.01
CH ₄	11.54	190.60	45.4	0.008	16.04
C ₂ -nC ₅	26.44	274.74	36.5	0.172	52.02
C ₆ -C ₁₀	38.09	438.68	25.1	0.284	103.01
C ₁₁₊	22.59	740.29	17.5	0.672	267.15

Table 3. Binary interaction coefficients for each component.

Component	CO ₂	N ₂	CH ₄	C ₂ -nC ₅	C ₆ -C ₁₀	C ₁₁₊
CO ₂	0	−0.020	0.1030	0.1299	0.1500	0.1500
N ₂	−0.020	0	0.0310	0.0820	0.1200	0.1200
CH ₄	0.1030	0.0310	0	0.0174	0.0462	0.1110
C ₂ -nC ₅	0.1299	0.0820	0.0174	0	0.0073	0.0444
C ₆ -C ₁₀	0.1500	0.1200	0.0462	0.0073	0	0.0162
C ₁₁₊	0.1500	0.1200	0.1110	0.0444	0.0162	0

In the base case, BHP of 1800 psi is the constraint for the production well at the beginning of the simulations. In the first three years, the well experiences a depletion production period. After that, it will be transferred to an injection well. The injection rate of CH₄ is set as 5000 Mscf/day. After 60 days of injection, the well will shut-in and begin a soaking period of 60 days. During the soaking period, the fluid is allowed to dissipate into the formation and mix with the fluid. Then the well is switched back on for another two-year production again. Thus, one cycle of CH₄ injection is finished. In this model, the production well experiences three cycles and the total production time is 15 years, as shown in Figure 5. A series of cases were conducted to simulate the cyclic CH₄ injection process. We compared the oil recovery factor in a 15-year period to investigate the effectiveness of CH₄ injection in the following sections.

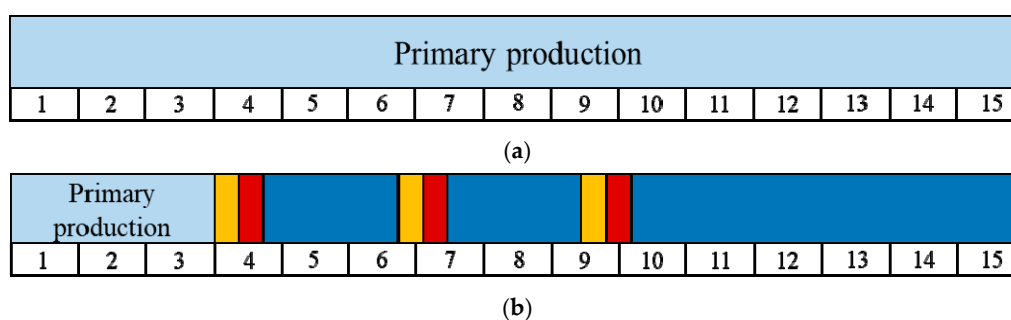


Figure 5. Production of different cases in total simulation time of 15 years: (a) Primary production; (b) Cyclic CH₄ injection (the yellow, red and dark blue bars represent CH₄ injection, soaking and EOR production period, respectively).

4. Results and Discussions

4.1. Effect of Confinement in Nanopores

The confinement is significant in the low permeability formations due to the nanopores. According to the experiment data from the Eagle Ford core samples [24], around 80% of the pores are 20 nm or less. The fluid properties under 5 nm, 10 nm, and 15 nm were calculated using the Equations (1) through (3), respectively, as listed in Table 4. The results show that critical temperatures and pressures suppress as the pore sizes reduce. With the procedure in Figure 2, we calculated the phase equilibrium and obtained the bubble point pressure under different pore sizes. As shown in Figure 6, the bubble

point pressure significantly decreases, especially for the small pores, which further impacts the oil recovery in the tight oil reservoirs.

Table 4. Critical temperatures and pressures under different pore sizes.

Components	Critical Temperatures (K)				Critical Pressures (Bar)			
	Bulk	15 nm	10 nm	5 nm	Bulk	15 nm	10 nm	5 nm
CO ₂	304.2	296.7	293.1	282.2	73.8	72.0	71.1	68.4
N ₂	126.2	123.2	121.7	117.4	33.9	33.1	32.7	31.6
CH ₄	190.6	185.9	183.6	176.8	46.0	44.9	44.3	42.7
C ₂ -nC ₅	274.7	266.6	262.5	250.6	37.0	35.9	35.3	33.7
C ₆ -C ₁₀	438.7	421.4	413.0	388.1	25.4	24.4	24.0	22.5
C ₁₁₊	740.3	701.4	682.4	627.0	17.7	16.8	16.3	15.0

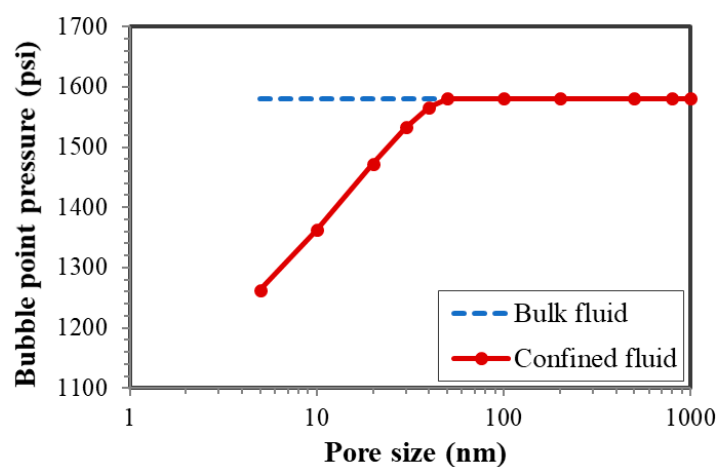


Figure 6. Bubble point pressure under different pore sizes.

Based on the pore size distribution of the formation, division of different pore regions are determined to represent the practical situation. Numbers of region ranging from 3 to 5 has been investigated and we finally decided 4 regions, which reduces computational cost and evaluates the confinement more reasonably. The contributions of each region are: less than 5 nm (42%), 5~10 nm (27%), 10~20 nm (13%), and larger than 20 nm (18%), respectively. The PVT properties of different pore sizes can be obtained in Section 2.1.

The effect of nanopore confinement on the well production was shown in Figure 7. It can be observed that the incremental oil recovery factor at the end of 15 years is 0.8% and 2.3% at the pore size of 10 nm and bulk, respectively, illustrating that the effect of confinement has a positive influence on the cyclic CH₄ injection effectiveness. Due to the confinement, the miscibility minimum pressure of the mixture and the oil viscosity decrease, leading to the improvement of well performance. Additionally, the bubble point pressure in the confined space is lower than the bulk phase, meaning that a longer time of single-phase production exist during the production. Hence, the confinement should be correctly included in the analysis of gas injection in the shale reservoirs. All the following cases include the confinement.

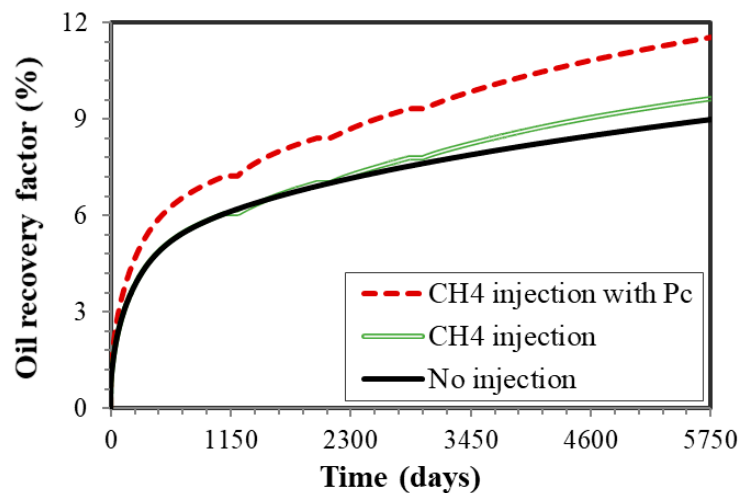


Figure 7. Effect of nanopore confinement on well performance in a 15-year period.

4.2. Molecular Diffusion

Molecular diffusion is another key parameter since CH_4 can move into the formation and mix with the oil during the soaking time. Neglecting diffusion coefficient will underestimate the ultimate oil recovery. In order to better analyze the mechanism of diffusion, we compared the oil recovery after 15 years with the coefficient ranging from $0.0001 \text{ cm}^2/\text{s}$ to $0.01 \text{ cm}^2/\text{s}$. As shown in Figure 8, the incremental oil recovery is 1.92%, 2.36%, and 2.98%, with the coefficients of 0.0001, 0.001, and $0.01 \text{ cm}^2/\text{s}$, respectively. The results indicate that more CH_4 molecules will diffuse into the matrix instead of concentrating around the fractures with larger diffusion coefficient. Hence, more oil will be swept, resulting in larger oil production.

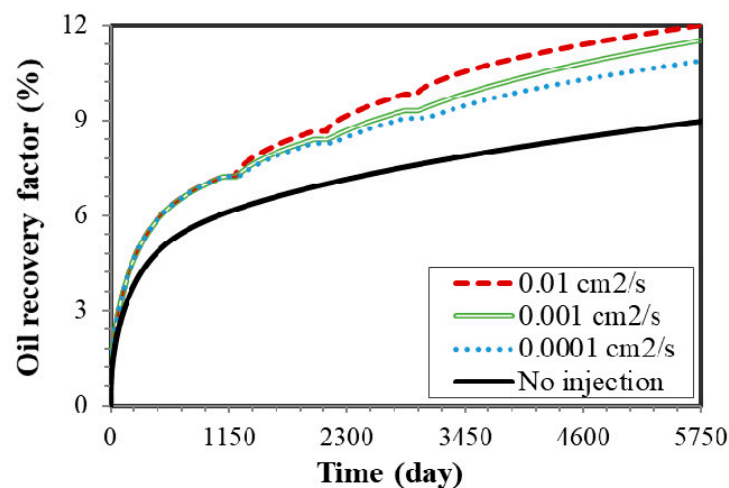


Figure 8. Effect of molecular diffusion on well production in a 15-year period.

4.3. Effect of Primary Depletion Period

The length of primary depletion period of 2, 3, and 5 years was studied, while other parameters were kept the same as the base case. As presented in Figure 9, the impact of primary depletion period is not noticeable since the increment is 2.28%, 2.34%, and 2.41%, respectively in this case. Delaying the start of gas injection is beneficial to improve the well production. However, if it starts too late, the production will decrease. Hence, decision of suitable primary depletion period is essential for the operations of CH_4 injection in the shale reservoirs.

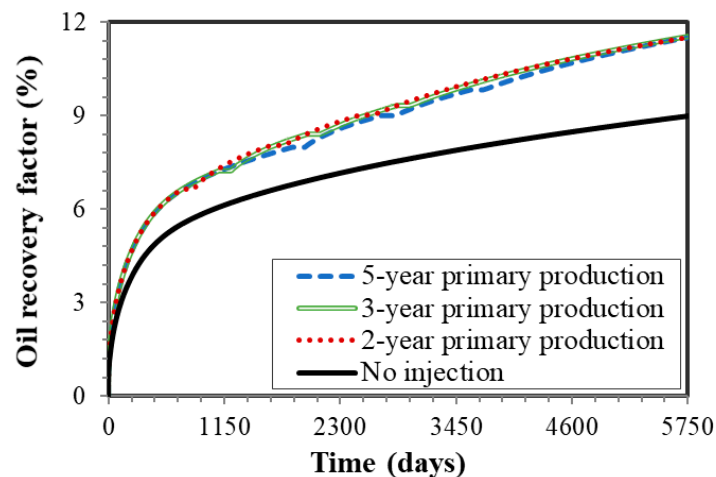


Figure 9. Comparison of oil recovery factor of different primary depletion period.

4.4. Effect of Injection Rate

Gas injection rate is directly related to the volume of CH_4 injected. A series of cases were conducted to investigate the effect of injection rate on the well performance of cyclic CH_4 injection. The rates were set as 2000, 5000, and 8000 Mscf/day, respectively. The results in Figure 10 show that the incremental oil recovery was 2.07%, 2.55%, and 2.82%, for the case of 2000, 5000, and 8000 Mscf/day, respectively, illustrating that higher injection rate leads to larger incremental oil recovery factor.

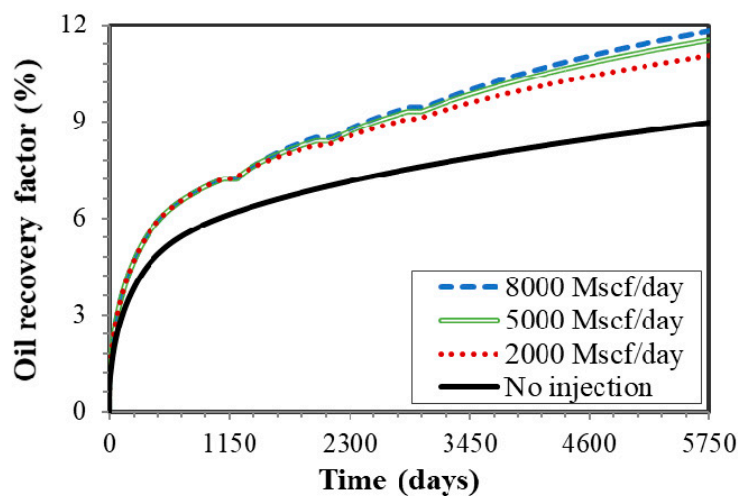


Figure 10. Comparison of oil recovery factor with different injection rates.

4.5. Effect of Injection Time

The length of injection time also impacts the CH_4 injection volume. We analyzed three cases with the injection time varying from 1 month to 3 months and kept other parameters as the same in the base case. As shown in Figure 11, oil recovery factor increases by 2.20%, 2.55%, and 2.76%, respectively. The results illustrate that longer injection time is beneficial to improve the efficiency of cyclic gas injection.

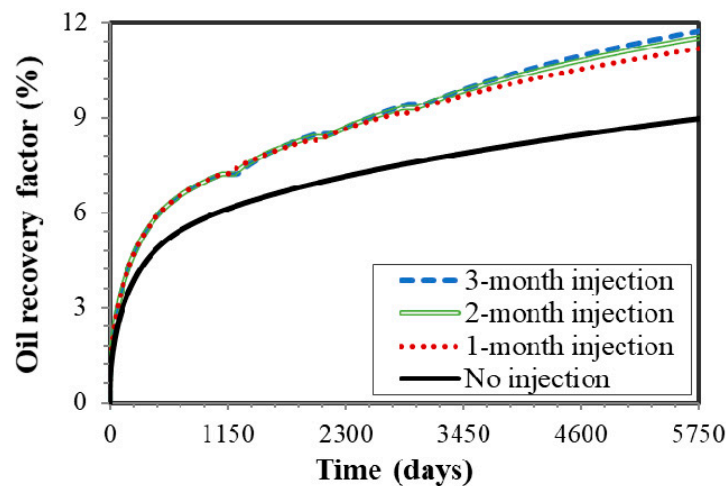


Figure 11. Comparison of oil recovery factor of different injection time.

4.6. Effect of Soaking Time

The soaking period affects the performance of Huff-n-Puff process as well. In this section, we conducted three cases with soaking time of 1 month, 2 months, and 3 months. As shown in Figure 12, the cases with the soaking time of 1 month, 2 months, and 3 months lead to the increment of 2.27%, 2.33%, and 2.37% after 15 years, respectively. As soaking period becomes longer, the CH_4 molecules will have more time to mix with oil phase adequately before its being produced back. Hence, the oil recovery factor improves with longer soaking time.

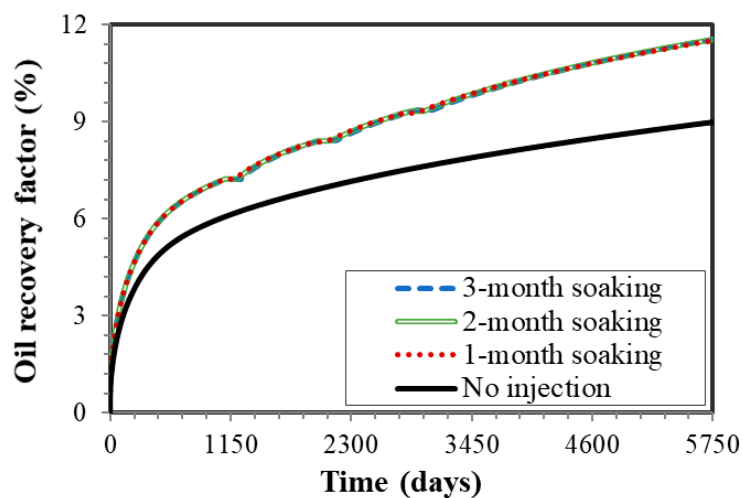


Figure 12. Comparison of oil recovery factor of different soaking time.

4.7. Effect of Number of Cycles

The number of cycles has significant impacts on the CH_4 injection effectiveness. We evaluated the well performance of the cases experiencing 1, 3, and 5 cycles, respectively. In Figure 13, compared the oil recovery factor of the scenarios with and without CH_4 injection for one-cycle treatment, the incremental oil recovery was boosted by 1.89%. Three-cycle processes yield the increment of 2.52%. For the five-cycle process, the incremental oil recovery is 2.72%. The increase of cycle numbers leads to the large incremental oil recovery; however, when it experiences 3 cycles or more, the impact on the well performance is diminished. Therefore, 3 cycles are suitable to reduce the operation cost and improve the oil production.

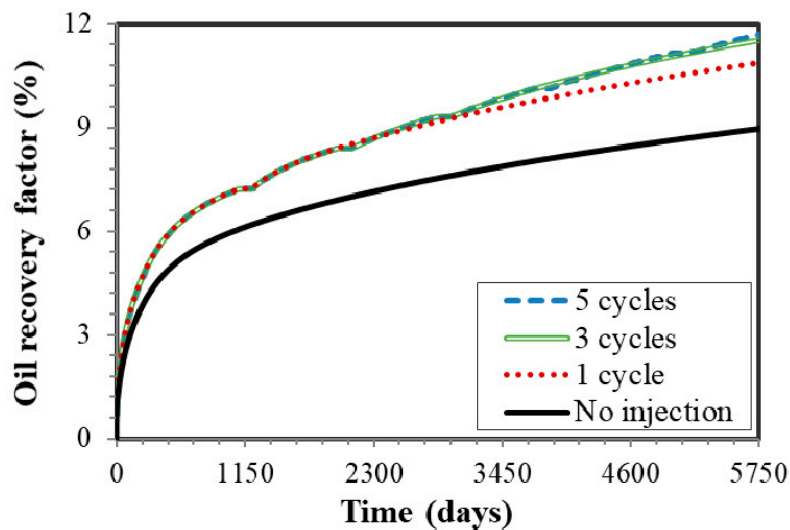


Figure 13. Comparison of oil recovery factor of different cycle treatments.

4.8. Effect of Matrix Permeability

In this section, we analyzed the effect of matrix permeability on the well performance. The matrix permeability was set ranging from 0.0001 mD to 0.01 mD. As shown in Figure 14, the oil recovery factor at the end of 15 years increases by 1.75%, 2.47% and 2.55%, corresponding to 0.0001, 0.001, and 0.01 mD, respectively. The matrix permeability influences the efficiency of CH_4 injection and higher permeability leads to larger incremental oil recovery. At the end of primary production, residual oil saturation is larger in the lower permeability formation and the diffusion mechanism is becoming more dominant. If the effect of confinement is included, more noticeable difference on the well performance will be observed in the higher permeability.

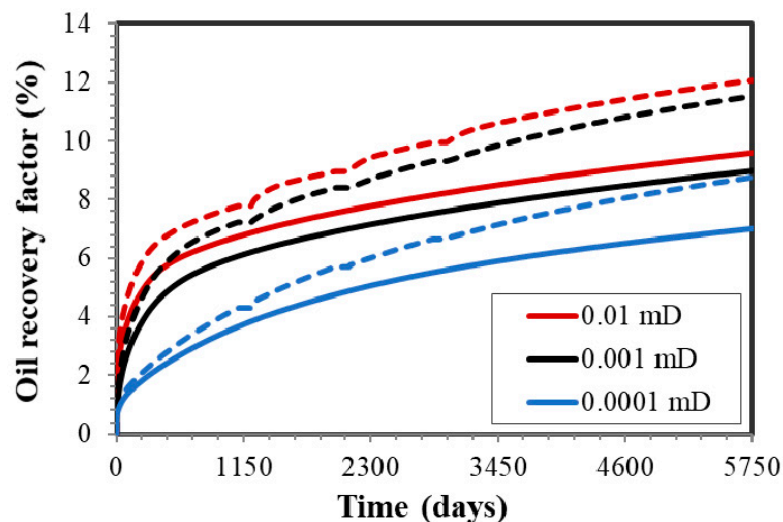
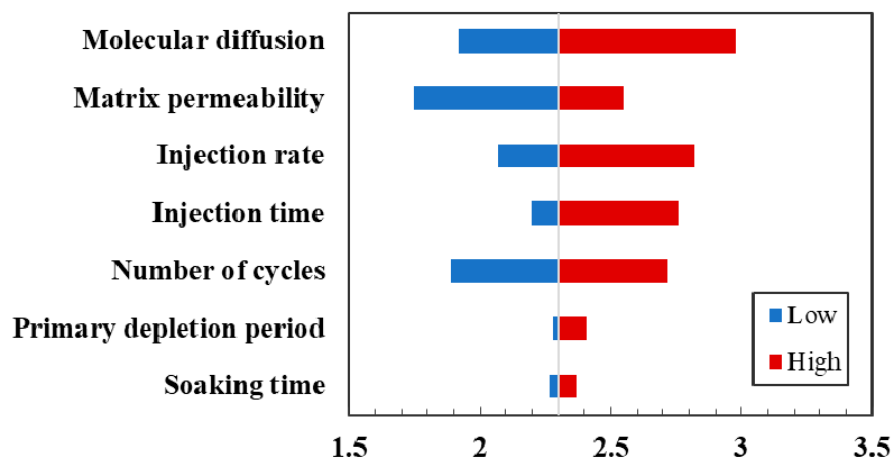


Figure 14. Effect of matrix permeability on oil recovery factor after 15 years (the solid and dash line represent the primary production and CH_4 injection, respectively).

We summarize the sensitivity parameters in Table 5 and represent by tornado plots shown in Figure 15. As shown, the most sensitive parameter for the cyclic CH_4 injection is the molecular diffusion, followed by matrix permeability, injection rate, injection time, and number of cycles. Primary depletion period and soaking time play the least important roles during the production time.

Table 5. Uncertain parameters and ranges for sensitivity analysis.

Parameters	Minimum	Medium	Maximum
Molecular diffusion/cm ² /s	0.0001	0.001	0.01
Primary depletion period/year	2	3	5
Injection time/day	30	60	90
Injection rate, Mscf/day	2000	5000	8000
Soaking time/day	30	60	90
Number of cycles	1	3	5
Matrix permeability, mD	0.001	0.01	0.1

**Figure 15.** Tornado plot for the sensitivity analysis.

5. Conclusions

In this study, a numerical model is proposed to investigate the cyclic CH₄ injection in the Eagle Ford shale incorporating physical mechanisms such as molecular diffusion and confinement in nanopores. The following conclusions can be drawn:

- (1) The effect of confinement in the nanopores is a significant factor in the simulation model to capture the real mechanism during the cyclic CH₄ injection;
- (2) A series of simulations were performed to evaluate the impacts of key parameters on the process of enhanced oil recovery, concluding that molecular diffusion is the most sensitive, followed by matrix permeability, injection rate, injection time, and number of cycles;
- (3) The impacts of primary depletion period and soaking time are less favorable for the cyclic CH₄ injection process;
- (4) This work provides a better understanding of factors affecting the efficiency of cyclic CH₄ injection, which can hopefully guide the operations in the shale reservoir.

Author Contributions: Conceptualization, Y.Z. and Y.D.; methodology and investigation Y.Z.; writing—original draft preparation, Y.Z.; writing—review and editing, J.H. and Y.S.; project administration, Y.D.; funding acquisition, Y.Z., Y.D. and J.H.

Funding: This research was funded by “National Natural Science Foundation of China, grant number 51804282 and 51674010”, “National Science and Technology Major Project of China, grant number 2017ZX05009-005”, “Fundamental Research Funds for the Central Universities, grant number 59/53200759016”, and “PetroChina Innovation Foundation (2017D-5007-0312)”.

Acknowledgments: We would like to appreciate Computer Modeling Group Ltd. for providing the CMG software for this investigation.

Conflicts of Interest: The authors declare no conflict of interest.

References

1. Salahshoor, S.; Fahes, M.; Teodoriu, C. A review on the effect of confinement on phase behavior in tight formations. *J. Nat. Gas Sci. Eng.* **2018**, *51*, 89–103. [[CrossRef](#)]
2. Mullen, J. Petrophysical characterization of the Eagle Ford shale in South Texas. In Proceedings of the Canadian Unconventional Resources & International Petroleum Conference, Calgary, AB, Canada, 19–21 October 2010.
3. Shelley, R.F.; Saugier, L.D.; Al-Tailji, W.; Guliyev, N.; Shah, K. Understanding hydraulic fracture stimulated horizontal Eagle Ford completions. In Proceedings of the SPE/EAGE European Unconventional Resources Conference and Exhibition, Vienna, Austria, 20–22 March 2012.
4. Zhang, L.; Kou, Z.; Wang, H.; Zhao, Y.; Dejam, M.; Guo, J.; Du, J. Performance analysis for a model of a multi-wing hydraulically fractured vertical well in a coalbed methane gas reservoir. *J. Pet. Sci. Eng.* **2018**, *166*, 104–120. [[CrossRef](#)]
5. Dejam, M.; Hassanzadeh, H.; Chen, Z. Semi-analytical solution for pressure transient analysis of a hydraulically fractured vertical well in a bounded dual-porosity reservoir. *J. Hydrol.* **2018**, *565*, 289–301. [[CrossRef](#)]
6. Xu, Z.H.; Zhao, P.Q.; Wang, Z.L.; Ostadhassan, M.; Pan, Z.H. Characterization and consecutive prediction of pore structures in tight oil reservoirs. *Energies* **2018**, *11*, 2705. [[CrossRef](#)]
7. Qian, K.; Yang, S.L.; Dou, H.E.; Wang, Q.; Wang, L.; Huang, Y. Experimental investigation on microscopic residual oil distribution during CO₂ Huff-and-Puff process in tight oil reservoirs. *Energies* **2018**, *11*, 2843. [[CrossRef](#)]
8. Dejam, M.; Hassanzadeh, H.; Chen, Z. Pre-Darcy flow in porous media. *Water Resour. Res.* **2017**, *53*, 8187–8210. [[CrossRef](#)]
9. Dejam, M.; Hassanzadeh, H.; Chen, Z. Pre-Darcy flow in tight and shale formations. In Proceedings of the 70th Annual Meeting of the APS (American Physical Society) Division of Fluid Dynamics, Denver, CO, USA, 19–21 November 2017.
10. Hawthorne, S.B.; Gorecki, C.D.; Sorensen, J.A.; Steadman, E.N.; Harju, A.J.; Melzer, S. Hydrocarbon mobilization mechanisms from upper, middle, and lower Bakken reservoir rocks exposed to CO₂. In Proceedings of the SPE Unconventional Resources Conference, Calgary, AB, Canada, 5–7 November 2013.
11. Ren, B.; Ren, S.; Zhang, L.; Chen, G.; Zhang, H. Monitoring on CO₂ migration in a tight oil reservoir during CCS-EOR in Jilin Oilfield China. *Energy* **2016**, *98*, 108–121. [[CrossRef](#)]
12. Sheng, J.J. Critical review of field EOR projects in shale and tight reservoirs. *J. Pet. Sci. Eng.* **2017**, *159*, 654–665. [[CrossRef](#)]
13. Wang, X.; Luo, P.; Er, V.; Huang, S.S. Assessment of CO₂ flooding potential for Bakken Formation, Saskatchewan. In Proceedings of the Canadian Unconventional Resources & International Petroleum Conference, Calgary, AB, Canada, 19–21 October 2010.
14. Sanchez-Rivera, D.; Mohanty, K.; Balhoff, M. Reservoir simulation and optimization of Huff-n-Puff operations in the Bakken shale. *Fuel* **2015**, *147*, 82–94. [[CrossRef](#)]
15. Alfarge, D.; Wei, M.; Bai, B. Feasibility of CO₂-EOR in shale-oil reservoirs: Numerical simulation study and pilot tests. In Proceedings of the Carbon Management Technology Conference, Houston, TX, USA, 17–20 July 2017.
16. Meng, X.; Yu, Y.; Sheng, J.J.; Watson, M.; Mody, F. An experimental study on huff-n-puff gas injection to enhance condensate recovery in shale gas reservoirs. In Proceedings of the Unconventional Resources Technology Conference, San Antonio, TX, USA, 20–22 July 2015.
17. Shi, R.; Kantzas, A. Enhanced heavy oil recovery on depleted long core system by CH₄ and CO₂. In Proceedings of the SPE International Thermal Operations and Heavy Oil Symposium, Calgary, AB, Canada, 20–23 October 2008.
18. Gamadi, T.D.; Elldakli, F.; Sheng, J.J. Compositional simulation evaluation of EOR potential in shale oil reservoirs by cyclic natural gas injection. In Proceedings of the Unconventional Resources Technology Conference, Denver, CO, USA, 25–27 August 2014.
19. Shen, Z.; Sheng, J.J. Experimental study of asphaltene aggregation during CO₂ and CH₄ injection in shale oil reservoirs. In Proceedings of the SPE Improved Oil Recovery Conference, Tulsa, OK, USA, 11–13 April 2016.

20. Sigmund, P.M.; Dranchuk, P.M.; Morrow, N.R.; Purvis, R.A. Retrograde condensation in porous media. *SPE J.* **1973**, *13*, 93–104. [[CrossRef](#)]
21. Brusilovsky, A.I. Mathematical simulation of phase behavior of natural multicomponent systems at high pressures with an equation of state. *SPE Res. Eng.* **1992**, *7*, 117–122. [[CrossRef](#)]
22. Du, L.; Chu, L. Understanding anomalous phase behavior in unconventional oil reservoirs. In Proceedings of the SPE Canadian Unconventional Resources Conference, Calgary, AB, Canada, 30 October–1 November 2012.
23. Nojabaei, B.; Johns, R.T.; Chu, L. Effect of capillary pressure on phase behavior in tight rocks and shales. *SPE Res. Eval. Eng.* **2013**, *16*, 281–289. [[CrossRef](#)]
24. Sanaei, A.; Jamili, A.; Callard, J.; Mathur, A. Production modeling in the Eagle Ford gas condensate window: Integrating new relationships between core permeability, pore size, and confined PVT properties. In Proceedings of the SPE Western North American and Rocky Mountain Joint Meeting, Denver, CO, USA, 16–18 April 2014.
25. Zhang, Y.; Lashgari, H.R.; Di, Y.; Sepehrnoori, K. Capillary pressure effect on hydrocarbon phase behavior in unconventional reservoirs. In Proceedings of the SPE Low Perm Symposium, Denver, CO, USA, 5–6 May 2016.
26. Wang, L.; Parsa, E.; Gao, Y.; Ok, J.T.; Neeves, K.; Yin, X.; Ozkan, E. Experimental study and modeling of the effect of nanoconfinement on hydrocarbon phase behavior in unconventional reservoirs. In Proceedings of the SPE Western North American and Rocky Mountain Joint Meeting, Denver, CO, USA, 16–18 April 2014.
27. Yang, G.; Fan, Z.; Li, X. Determination of confined fluid phase behavior using modified Peng-Robinson equation of state. In Proceedings of the Unconventional Resources Technology Conference, Houston, TX, USA, 23–25 July 2018.
28. Luo, S.; Nasrabadi, H.; Lutkenhaus, J.L. Effect of confinement on the bubble points of hydrocarbons in nanoporous media. *AIChE J.* **2016**, *62*, 1772–1780. [[CrossRef](#)]
29. Alfi, M.; Nasrabadi, H.; Banerjee, D. Effect of confinement on bubble point temperature shift of hydrocarbon mixtures: Experimental investigation using nanofluidic devices. In Proceedings of the SPE Annual Technical Conference and Exhibition, San Antonio, TX, USA, 9–11 October 2017.
30. Yu, W.; Lashgari, H.R.; Wu, K.; Sepehrnoori, K. CO₂ injection for enhanced oil recovery in Bakken tight oil reservoirs. *Fuel* **2015**, *159*, 354–363. [[CrossRef](#)]
31. Du, X.D.; Gu, M.; Duan, S.; Xian, X.F. Investigation of CO₂–CH₄ displacement and transport in shale for enhanced shale gas recovery and CO₂ sequestration. *J. Energy Resour. Technol.* **2017**, *139*, 012909. [[CrossRef](#)]
32. Zhang, Y.; Yu, W.; Li, Z.; Sepehrnoori, K. Simulation study of factors affecting CO₂ Huff-n-Puff process in tight oil reservoirs. *J. Pet. Sci. Eng.* **2018**, *163*, 264–269. [[CrossRef](#)]
33. Wu, K.; Li, X.; Guo, C.; Wang, C.; Chen, Z. A unified model for gas transfer in nanopores of shale-gas reservoirs: Coupling pore diffusion and surface diffusion. *SPE J.* **2016**, *21*, 1583–1611. [[CrossRef](#)]
34. Chen, C.; Gu, M. Investigation of cyclic CO₂ huff-and-puff recovery in shale oil reservoirs using reservoir simulation and sensitivity analysis. *Fuel* **2017**, *188*, 102–111. [[CrossRef](#)]
35. Simpson, M.D.; Patterson, R.; Wu, K. Study of stress shadow effects in Eagle Ford Shale: Insight from field data analysis. In Proceedings of the 50th U.S. Rock Mechanics/Geomechanics Symposium, American Rock Mechanics Association, Houston, TX, USA, 26–29 June 2016.
36. Singh, S.K.; Sinha, A.; Deo, G.; Singh, J.K. Vapor-liquid phase coexistence, critical properties, and surface tension of confined alkanes. *J. Phys. Chem. C* **2009**, *113*, 7170–7180. [[CrossRef](#)]
37. Jin, L.C.; Ma, Y.X.; Jamili, A. Investigating the effect of pore proximity on phase behavior and fluid properties in shale formations. In Proceedings of the SPE Annual Technical Conference and Exhibition, New Orleans, LA, USA, 30 September–2 October 2013.
38. Campos, M.D.; Akkutlu, I.Y.; Sigal, R.F. A molecular dynamics study on natural gas solubility enhancement in water confined to small pores. In Proceedings of the SPE Annual Technical Conference and Exhibition, New Orleans, LA, USA, 4–7 October 2009.
39. Devegowda, D.; Sapmanee, K.; Civan, F.; Sigal, R.F. Phase behavior of gas condensates in shales due to pore proximity effects: Implications for transport, reserves and well productivity. In Proceedings of the SPE Annual Technical Conference and Exhibition, San Antonio, TX, USA, 8–10 October 2012.
40. Zarragoicochea, G.J.; Kuz, V.A. Critical shift of a confined fluid in a nanopore. *Fluid Phase Equilib.* **2004**, *220*, 7–9. [[CrossRef](#)]

41. Adamson, A.W. Capillarity. In *Physical Chemistry of Surfaces*, 5th ed.; John Wiley & Sons: New York City, NY, USA, 1990.
42. Pedersen, K.S.; Christensen, P.L. Flash and phase envelope calculations. In *Phase Behavior of Petroleum Reservoir Fluids*, 1st ed.; CRC Press Taylor & Francis Group: Boca Raton, FL, USA, 2006.
43. Peng, D.Y.; Robinson, D.B. A new two-constant equation of state. *Ind. Eng. Chem. Fundam.* **1976**, *15*, 59–64. [[CrossRef](#)]
44. CMG. *GEM-GEM User's Guide*; Computer Modeling Group Ltd.: Calgary, AB, Canada, 2012.
45. Condon, S.M.; Dyman, T.S. *Geologic Assessment of Undiscovered Conventional Oil and Gas Resources in the Upper Cretaceous Navarro and Taylor Groups, Western Gul Province*; Texas: USGS Digital Data Series; USGU: Reston, VA, USA, 2006.
46. Mohebbinia, S.; Wong, T. Molecular diffusion calculations in simulation of gasfloods in fractured reservoirs. In Proceedings of the SPE Reservoir Simulation Conference, Montgomery, AL, USA, 20–22 February 2017.
47. Orangi, A.; Nagarajan, N.R.; Honarpour, M.M.; Rosenzweig, J.J. Unconventional shale oil and gas-condensate reservoir production, impact of rock, fluid, and hydraulic fractures. In Proceedings of the SPE Hydraulic Fracturing Technology Conference and Exhibition, The Woodlands, TX, USA, 24–26 January 2011.



© 2018 by the authors. Licensee MDPI, Basel, Switzerland. This article is an open access article distributed under the terms and conditions of the Creative Commons Attribution (CC BY) license (<http://creativecommons.org/licenses/by/4.0/>).